

## Simultaneous diffusion of Si and N in silicon nitride

H. Schmidt

*TU Clausthal, Fakultät für Natur- und Materialwissenschaften, Thermochemie und Mikrokinetik, Robert-Koch-Strasse 42, D-38678 Clausthal-Zellerfeld, Germany*

U. Geckle and M. Bruns

*Forschungszentrum Karlsruhe GmbH, Institut für Materialforschung III, Hermann-von-Helmholtz-Platz 1, D-76344 Eggenstein-Leopoldshafen, Germany*

(Received 5 April 2006; published 12 July 2006)

Silicon nitride is a covalently bound solid of scientific and technological importance with a very low atomic mobility where reliable self-diffusivities are still lacking. We used  $^{28}\text{Si}_3^{14}\text{N}_4/\text{nat}\text{Si}_3^{15}\text{N}_4/^{28}\text{Si}_3^{14}\text{N}_4$  isotope heterostructures produced by reactive magnetron sputtering and subsequent *in situ* crystallization in combination with secondary ion mass spectrometry to study self-diffusion. Si and N diffusivities were measured in polycrystalline  $\alpha\text{-Si}_3\text{N}_4$  by isotope interdiffusion at temperatures between 1200 and 1700 °C. The diffusivities of the two elements coincide within error limits over the whole temperature range investigated and follow an Arrhenius law with an activation enthalpy of  $\Delta H=5.0$  eV and a pre-exponential factor of  $D_0=6\times 10^{-6}$  m<sup>2</sup>/s. Isotope heterostructures which are composed of a phase mixture of  $\alpha\text{-Si}_3\text{N}_4$  and  $\beta\text{-Si}_3\text{N}_4$  show diffusivities which are not significantly lower and which have nearly the same activation enthalpy of  $\Delta H=4.9$  eV, indicating similar diffusivities in both polymorphic phases of silicon nitride. The entropy of self-diffusion is calculated to  $\Delta S\approx 2 k_B$ , which is a hint that diffusion is mediated by localized point defects, in contrast to extended point defects usually found in other semiconductors, such as Si, Ge, and GaAs. Possible diffusion mechanisms are discussed.

DOI: [10.1103/PhysRevB.74.045203](https://doi.org/10.1103/PhysRevB.74.045203)

PACS number(s): 66.30.Hs

### I. INTRODUCTION

Silicon nitride ( $\text{Si}_3\text{N}_4$ ) is a compound with an excellent high temperature stability (up to 1900 °C at ambient pressure) which exhibits a variety of attractive properties, such as high hardness, chemical stability, high thermal shock resistance, a good creep behavior, and a good oxidation resistance. In addition, this material is also a wide band gap semiconductor usable for electronic applications in the form of thin films. These properties suggest mechanical, optical, and electronic applications in various branches of technology.<sup>1-5</sup> Silicon nitride exhibits two crystalline polymorphs,  $\alpha\text{-Si}_3\text{N}_4$  (space group *P31c*) and  $\beta\text{-Si}_3\text{N}_4$  (space group *P63/m*), respectively, where the latter one is assumed to be the stable phase and the first one a metastable modification.<sup>3</sup> The basic building unit of the crystal structure is a silicon-nitrogen tetrahedron in which a silicon atom lies in the center and four nitrogen atoms at each corner.<sup>3</sup> The  $\text{SiN}_4$  tetrahedra are joined in such a way that each nitrogen is common to three tetrahedra in order to form a three-dimensional structure. The predominantly covalent bonds are the reason for a very low atomic mobility in this material, which is a prerequisite for its thermal stability. Despite its technological and scientific importance, no systematic studies were carried out on the self-diffusion of the two constituting elements. Such studies will help to explain the thermal stability, the dissociation, and the high temperature mechanical properties of this material. From a fundamental point of view, these studies will also contribute to a better understanding of point defect motion in covalently bound solids, which is not very well characterized.<sup>6</sup>

The lack of self-diffusion experiments is due to the fact that the compound requires advanced methods to determine

reliable diffusion data. The special problems arising for  $\text{Si}_3\text{N}_4$  and the strategies to overcome these problems are summarized here: (1) For the two constituting elements, no suitable radioactive tracers are available for the performance of extensive measurements. This fact prevents the use of the radiotracer technique with its high detection sensitivity which is state-of-the-art in diffusivity determination. Consequently, the stable isotopes ( $^{14}\text{N}$ ,  $^{15}\text{N}$ ) and ( $^{28}\text{Si}$ ,  $^{29}\text{Si}$ ,  $^{30}\text{Si}$ ) have to be used as tracers. (2) The lack of large bulk  $\text{Si}_3\text{N}_4$  single crystals and the presence of glassy, often impurity contaminated, intergranular phase in sintered or hot-pressed polycrystalline material considerably complicates self-diffusion measurements in bulk material. This problem is overcome by the use of magnetron sputtered  $\text{Si}_3\text{N}_4$  thin films which are nearly impurity free. (3) The existence of very low diffusivities even at high temperatures and the geometry of thin films limited to the submicrometer range necessitates the application of analytical methods with an excellent depth resolution, such as secondary ion mass spectrometry (SIMS). (4) Surface effects, such as oxidation, may influence the tracer deposition and the diffusion process substantially. Here, the deposition of the tracer beyond the surface, in the interior of the sample, is preferred. The existence of these problems is also reflected in the fact that in literature only a very limited number of publications on self-diffusion in silicon nitride exist<sup>7,8</sup> whose results are hardly convincing. In this study, so-called isotope heterostructures were used to overcome the described problems and to quantify self-diffusivities in silicon nitride by simultaneous diffusion of Si and N. Isotope heterostructures are nanoscaled isotope-enriched layers of the form  $^{28}\text{Si}_3^{14}\text{N}_4/\text{nat}\text{Si}_3^{15}\text{N}_4/^{28}\text{Si}_3^{14}\text{N}_4$ , which are produced by reactive magnetron sputtering on a

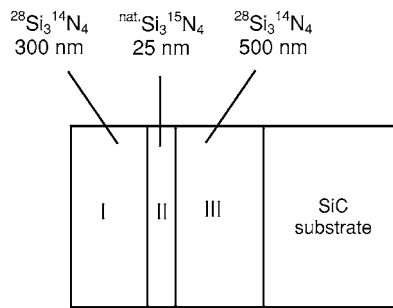


FIG. 1. Schematic sketch of a silicon nitride isotope heterostructure deposited on a SiC substrate, as used in this work.

high temperature stable SiC substrate. During annealing at elevated temperatures, isotope interdiffusion takes place without changing the chemical composition. The diffusivities are determined by isotope depth profiling with SIMS.

## II. EXPERIMENTAL

In the present work, the self-diffusion of Si and N in crystalline silicon nitride is investigated using isotope enriched layers of the form  $^{28}\text{Si}_3^{14}\text{N}_4/\text{nat}\text{Si}_3^{15}\text{N}_4/^{28}\text{Si}_3^{14}\text{N}_4$  with approximate dimensions of about 300 nm/25 nm/500 nm (isotope heterostructures). Such an isotope heterostructure is schematically sketched in Fig. 1. Here, the tracer is introduced into the system *in situ* during synthesis by depositing the consecutive layers I, II, and III by reactive rf magnetron sputtering. A mixture of 50 vol. % argon and 50 vol. % nitrogen, either nitrogen with natural isotope content ( $^{14}\text{N}$  concentration, 99.63%) or isotopically enriched nitrogen ( $^{15}\text{N}$  concentration, 99.5%) was used in combination with different isotope enriched silicon targets. For layer II a conventional Si target (Norwegian Talc, Germany) with a natural abundance of the Si isotopes ( $^{28}\text{Si}$ , 92.2%;  $^{29}\text{Si}$ , 4.7%;  $^{30}\text{Si}$ , 3.1%) was used with  $^{15}\text{N}$  enriched sputter gas. In contrast, for layer I and III a  $^{28}\text{Si}$  enriched silicon target ( $^{28}\text{Si}$  concentration, 99.9%) (Isonics Corp., USA) is used with  $^{14}\text{N}$  gas. During annealing of the heterostructures, layer II serves as a tracer layer and the diffusion of the  $^{30}\text{Si}$  and  $^{15}\text{N}$  isotopes into the silicon nitride layers I and III is investigated.

Magnetron sputter deposition was achieved using a 3 in. US GUN low profile planar magnetron source (AP&T, Nürtingen, Germany) mounted on a standard DN 150 CF double-cross recipient equipped with presputter shutter and sample positioner. Deposition rates of 2–5 nm/min are achieved, using an operating pressure of  $5 \times 10^{-3}$  mbar and a sputtering power of 160 W at a substrate temperature of 400 °C. As substrates, polycrystalline SiC (BCS, Germany) was preferred to Si wafers to ensure a high temperature stability of the system over 1400 °C and to enable an *in situ* crystallization of the amorphous as-deposited heterostructures in order to investigate diffusion in the crystalline state. The substrates ( $10 \times 10 \times 2$  mm<sup>3</sup>) were polished with diamond paste down to a surface roughness smaller than 5 nm and cleaned with ethanol.

The isotope heterostructures were diffusion annealed in a silicon nitride powder pack in the temperature range between

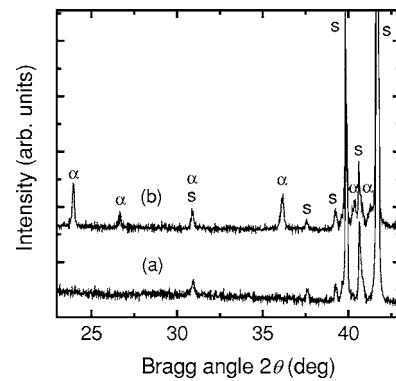


FIG. 2. X-ray diffractograms of a  $^{28}\text{Si}_3^{14}\text{N}_4/\text{nat}\text{Si}_3^{15}\text{N}_4/^{28}\text{Si}_3^{14}\text{N}_4$  heterostructure in the as-deposited state (a) and after annealing for 2 h at 1500 °C (b) where  $\alpha$ - $\text{Si}_3\text{N}_4$  is formed. Peaks referring to  $\alpha$ - $\text{Si}_3\text{N}_4$  are marked with an  $\alpha$  and those referring to the SiC substrate are marked with an  $s$ .

1200 and 1700 °C in nitrogen at ambient pressure. Tracer depth profiles of  $^{14}\text{N}^+$ ,  $^{15}\text{N}^+$ ,  $^{28}\text{Si}^+$ ,  $^{29}\text{Si}^+$ , and  $^{30}\text{Si}^+$  were measured by SIMS (CAMECA IMS-3F) using an  $\text{O}^-$  ion beam. In order to prevent electrical charging during the measurement, the insulating samples were coated with a thin layer of gold before SIMS analysis. Depth calibration was obtained by measuring the crater depth with a mechanical profilometer.

## III. RESULTS

The elemental composition of the sputtered isotope heterostructures was measured by non-Rutherford backscattering spectroscopy (n-RBS) at the Institut für Kernphysik (Universität Frankfurt, Germany). The simulation of the n-RBS spectrum with the computer code RUMP (Ref. 9) demonstrates that the film consists of stoichiometric  $\text{Si}_3\text{N}_4$  (an example of such a spectrum can be found in Ref. 10). The O impurity concentration was determined with the same method to be less than 0.2 at % indicating the high purity of the material. As can be seen in Fig. 2, the isotope heterostructures are x-ray amorphous after deposition. In order to form polycrystalline silicon nitride, a thermal treatment of 2 h at 1500 °C was applied, which results in complete crystallization. Details on the crystallization process and the underlying kinetics can be found in Ref. 11. As visible in Fig. 2, the *in situ* crystallized isotope heterostructures investigated in this study show only x-ray peaks corresponding to  $\alpha$ - $\text{Si}_3\text{N}_4$ . The absence of any  $\beta$ - $\text{Si}_3\text{N}_4$  peak indicates a fraction of this phase below 3%, which is the detection limit of this method. The crystallite size was determined to about 80 nm from the full width at half maximum of the x-ray peaks.

Examples of  $^{15}\text{N}$  isotope depth profiles as obtained by SIMS analysis of as-deposited and crystallized isotope heterostructures, respectively, are given in Fig. 3. The width of the  $^{15}\text{N}$  SIMS signal which results from layer II in Fig. 1 is slightly broadened from about 25 nm to about 40 nm during the crystallization process. This broadening is due to the atomic rearrangement processes governing crystallization.

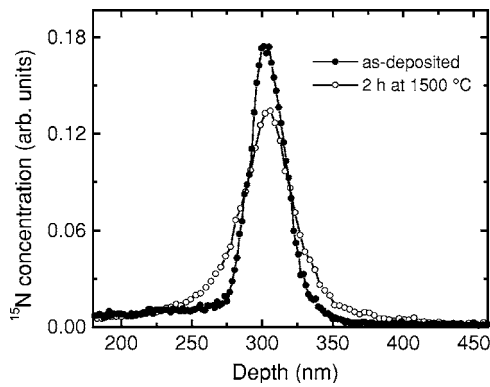


FIG. 3.  $^{15}\text{N}$  SIMS depth profiles measured on a  $^{28}\text{Si}_3^{14}\text{N}_4/\text{natSi}_3^{15}\text{N}_4/^{28}\text{Si}_3^{14}\text{N}_4$  isotope heterostructure after deposition and after additional annealing for 2 h at 1500 °C corresponding to crystallization.

However, the regions I, II, and III are well separated and the profile measured after crystallization can reliably be used as a starting profile for subsequent diffusion experiments. In Fig. 4 examples of  $^{15}\text{N}$  and  $^{30}\text{Si}$  depth profiles are given for a sample which was additionally diffusion annealed after crystallization at a temperature of 1400 °C for 64 h. Further broadening of the starting profile due to diffusion is obvious for both elements, which enables the simultaneous determination of Si and N diffusivities during a single measurement. After diffusion annealing, the x-ray diffraction (XRD) diagrams do not show any modification, indicating a stable crystalline state and no further structural changes. Assuming a step function for the interfaces in the as-deposited structure, experimental profiles broadened after annealing can be described with the following solution of Fick's second law for self-diffusion across an interface:

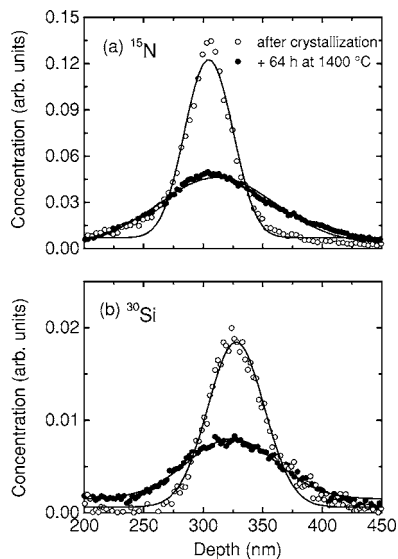


FIG. 4. (a)  $^{15}\text{N}$  depth profiles and (b)  $^{30}\text{Si}$  depth profiles measured on  $^{28}\text{Si}_3^{14}\text{N}_4/\text{natSi}_3^{15}\text{N}_4/^{28}\text{Si}_3^{14}\text{N}_4$  isotope heterostructures after preannealing for 2 h at 1500 °C (crystallization) and after additional diffusion annealing for 64 h at 1400 °C. The solid lines correspond to a least-squares fit of the experimental data to Eq. (1). The background is subtracted for clarity.

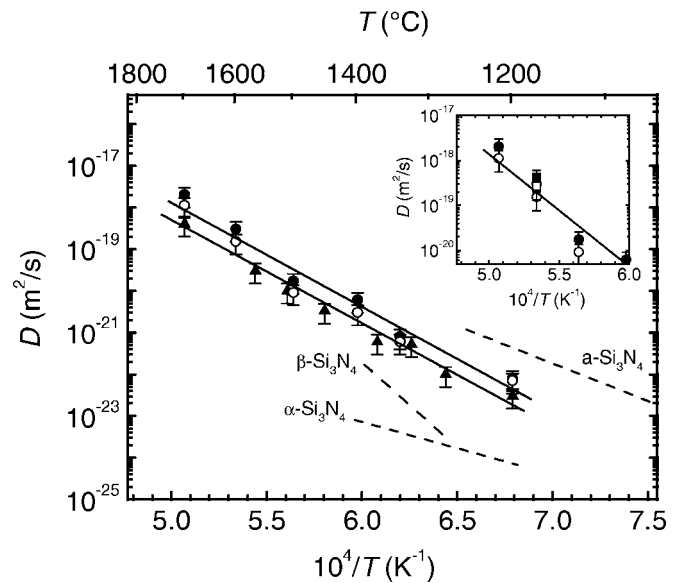


FIG. 5. N (●) and Si (○) diffusivities in polycrystalline  $\alpha\text{-Si}_3\text{N}_4$  as a function of reciprocal temperature as obtained by annealing in nitrogen at ambient pressure. Also shown are N diffusivities of isotope heterostructures consisting of a mixture of  $\alpha\text{-Si}_3\text{N}_4$  and  $\beta\text{-Si}_3\text{N}_4$  (▲) (according to Ref. 10), N diffusivities measured on polycrystalline powders by Kijima and Shirasaki (dashed lines),<sup>7</sup> and N diffusivities in amorphous silicon nitride ( $a\text{-Si}_3\text{N}_4$ , dashed line).<sup>20</sup> The enlarged inset shows additional N (■) and Si (□) diffusivities at 1600 °C which were obtained by a diffusion annealing in argon atmosphere (nitrogen partial pressure about 1 mbar).

$$c(x, t) = c_\infty + \frac{(c_0 - c_\infty)}{2} \left[ \text{erf}\left(\frac{x-l}{R}\right) + \text{erf}\left(\frac{h+l-x}{R}\right) \right], \quad (1)$$

where  $c_\infty$  is the concentration of  $^{15}\text{N}$  or  $^{30}\text{Si}$  in layer I and III, and  $c_0$  in the tracer layer II, respectively. The original thickness of the tracer layer is denoted as  $h$  and the thickness of the top layer as  $l$ . Since the isotope concentration is proportional to the intensity of the secondary ions produced during SIMS analysis, we can apply Eq. (1) directly to our measurement data. The quantity  $R$ , describing the broadening of the tracer profile, is treated as a fitting parameter. The self-diffusivity  $D$  at time  $t$  is determined from the difference in  $R$  of the diffusion profile and of the starting profile according to  $D = [R^2(t) - R^2(0)]/4t$ .<sup>12</sup>

The determined Si and N diffusivities are given in Fig. 5, presented as a function of reciprocal temperature. Very low diffusivities down to  $10^{-23}$   $\text{m}^2/\text{s}$  are obtained in the temperature range between 1200 and 1700 °C. These values are typically several orders of magnitude lower than for metals<sup>13</sup> (e.g., the self-diffusivity of vanadium is about five orders of magnitude higher than that of the silicon nitride constituents at 1700 °C, while the melting and decomposition temperature of both materials coincide at 1900 °C). The reason for the slow diffusion is the presence of covalent Si-N bond bonds with a high dissociation energy of 3.48 eV (Ref. 3), which has at least to be overcome during atomic motion. From Fig. 5 it is also obvious that the Si and N diffusivities

TABLE I. Activation enthalpies and pre-exponential factors for the self-diffusivities in polycrystalline silicon nitride. For details see text.

Material	Diffusing element	$\Delta H$ (eV)	$\text{Log}_{10}D_0$
$\text{Si}_3\text{N}_4$ ( $\alpha$ phase)	Si	$4.9 \pm 0.4$	$-5.7 \pm 1.4$
$\text{Si}_3\text{N}_4$ ( $\alpha$ phase)	N	$5.2 \pm 0.4$	$-4.6 \pm 1.3$
$\text{Si}_3\text{N}_4$ ( $\alpha$ phase)	Si+N	$5.0 \pm 0.3$	$-5.2 \pm 0.9$
$\text{Si}_3\text{N}_4$ ( $\alpha+\beta$ phase) <sup>a</sup>	N	$4.9 \pm 0.4$	$-6.0 \pm 1.2$

<sup>a</sup>Reference 10.

do not deviate much if compared for the same temperature. The Si diffusivities are smaller by a factor of about 1.5 in the temperature range investigated. For a closer inspection, the experimental errors attributed to a diffusivity needs further consideration. The overall relative error given in Fig. 5 was determined to be about 50% and is mainly caused by the accuracy of the depth measurement of the SIMS crater and by the averaging of several measurements carried out on one sample (typically 2–3). However, if the Si and N diffusivities are compared at the same temperature, the error limits attributed to each data point are smaller. Since both diffusivities were obtained during the identical SIMS measurement, crater depth measurement and averaging do not contribute to the error in this case. Consequently, a smaller relative error of only 20% can be assigned, resulting from the least-squares fitting procedure of the experimental data to Eq. (1). With these assumption, the slightly lower diffusivities of Si can be attributed to the higher mass,  $m$ , of this element. Using the relation  $D \sim m^{-1/2}$  and a relative mass of 30 a.u. for Si and 15 a.u. for N, Si diffusivities which are lower by a factor of 1.4 can be expected, as experimentally observed (considering an error of 20%). From these observations it can be concluded that the Si and N diffusivities are identical, if they are corrected for the mass effect.

For further analysis, an Arrhenius equation,

$$D = D_0 \exp(-\Delta H/k_B T), \quad (2)$$

is used to describe the experimental data. A common least-squares fit of Eq. (2) to the N and Si diffusivities results in an activation enthalpy of  $\Delta H = (5.0 \pm 0.3)$  eV and a pre-exponential factor of  $D_0 = 6 \times 10^{-6} \text{ m}^2/\text{s}$  (error:  $\log_{10} D_0 = \pm 0.9$ ). Both parameters do not change within error limits, if the N or Si diffusivities are fitted separately or the mass corrected Si diffusivities are used instead of the original data (see Table I).

Investigations on the nitrogen diffusion in silicon nitride, where a mixture of the polymorphic modifications  $\alpha$ - $\text{Si}_3\text{N}_4$  (60–70%) and  $\beta$ - $\text{Si}_3\text{N}_4$  (30–40%) are present after crystallization were also carried out by our group (however with  $^{15}\text{N}$  enriched isotope heterostructures only). Preliminary results were recently published in the form of a letter.<sup>10</sup> The isotope depth profiles (for example, see Fig. 2 in Ref. 10) do not differ significantly from those shown in Figs. 3 or 4, and were also least-squares fitted by Eq. (1). No asymmetric profile shapes and no significant deviations from the fitting

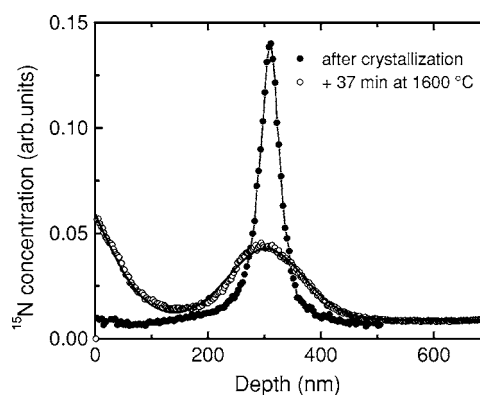


FIG. 6.  $^{15}\text{N}$  depth profile of an isotope heterostructure after annealing for 37 min at 1600 °C. The lines correspond to a fit of the experimental data to Eq. (3). For more details, see the text.

curve are observed, indicating that the presence of the two phases is not reflected in the diffusion profiles. The N diffusivities are also shown in Fig. 5, where only small differences are observed for the single-phase and two-phase materials. The diffusivities of the two-phase samples are lower by a maximum factor of only 5, which is close to the limit of estimated errors. Consequently a similar activation enthalpy of  $\Delta H = (4.9 \pm 0.4)$  eV and a similar pre-exponential factor of  $D_0 = 1 \times 10^{-6} \text{ m}^2/\text{s}$  is determined by least-squares fitting. These results indicate that self-diffusion is almost identical in both crystalline modifications of silicon nitride, in contrast to prior publications.<sup>7</sup>

The enlarged inset of Fig. 5 shows additional Si and N diffusivities at 1600 °C that were determined from isotope heterostructures, which were diffusion annealed at a reduced nitrogen partial pressure. Instead of using 960 mbar of pure nitrogen gas, the diffusion experiments were carried out in a mixture of 1 mbar of nitrogen and 959 mbar of argon. As obvious the diffusivities at 1600 °C are identical for both types of experiments. This means that diffusion at this temperature is not influenced by nitrogen partial pressure, which is a strong indication that the system is not coupled to the environment (also at high temperatures). Consequently, very likely no formation of structural defects occurs by reaction with the gas atmosphere and the exact chemical composition of the sample in the homogeneity range of silicon nitride is determined by the deposition and crystallization procedure.

As mentioned before, the isotope heterostructures are polycrystalline. This means that diffusional transport may take place in volume (as already discussed) or in grain boundaries. Due to the relatively small penetration depth of the measured diffusion profiles of less than 50 nm and due to an average grain diameter of about 80 nm, only a minor amount of tracer is present in grain boundaries (less than 2%) and grain boundary transport does not contribute significantly to the observed broadened diffusion profiles. Possible grain boundary diffusion profiles are masked by the natural background of  $^{15}\text{N}$  and  $^{30}\text{Si}$  isotopes in layers I and III. However, the influence of grain boundaries is indirectly reflected in the depth profiles at high temperatures ( $>1500$  °C). In Fig. 6  $^{15}\text{N}$  depth profiles are plotted over the whole film thickness of a heterostructure which was annealed at

1600 °C for 37 min. In addition to the broadened isotope enriched layer II, a strong increase of the  $^{15}\text{N}$  concentration is observed close to the surface. Similar observations were made for  $^{30}\text{Si}$  tracers. A plausible explanation for this observation can be found under the assumption that diffusion along grain boundaries takes place parallel to volume diffusivity, however, with a much higher diffusivity. Consequently, during annealing a significant amount of  $^{15}\text{N}$  tracer can be transported along the grain boundaries from the tracer layer to the sample surface. Due to the small amount of tracer present in the grain boundaries, the profile broadening of layer II corresponding to this transport is masked by the natural isotope background. At the surface, the adsorbed tracer atoms are homogeneously distributed over the surface due to fast surface diffusion. From this reservoir, the tracer can now penetrate again into the grains of the film by volume diffusion. In principle, the tracer reservoir at the surface is a continuous source which is supplied from the  $^{15}\text{N}$  reservoir in the interior of the heterostructure. The depth profile can be fitted (see Fig. 6) with the equation

$$c(x,t) = c_\infty + \frac{(c_0 - c_\infty)}{2} \left[ \operatorname{erf}\left(\frac{x-l}{R}\right) + \operatorname{erf}\left(\frac{h+l-x}{R}\right) \right] + c_s \operatorname{erfc}\left(\frac{x}{2\sqrt{Dt}}\right), \quad (3)$$

which is the sum of Eq. (1) and of the solution of Fick's law for an infinite source present at the surface.<sup>12</sup> Here,  $c_s$  is the concentration of the tracer at the sample surface and the other parameters have their usual meaning. If the volume diffusivity,  $D$ , is used as a fitting parameter (and also  $c_0$ ), the obtained values are identical within errors to those derived from the conventional fitting procedure using only Eq. (1) on the broadening of layer II.

The number of  $^{15}\text{N}$  tracer atoms present in a heterostructure can be obtained by numerically integrating the  $^{15}\text{N}$  profile over depth after subtracting the background. This procedure carried out for both profiles in Fig. 6 revealed that the number of tracer atoms does not change during diffusion, excluding an evaporation of the tracer. Further, the number of tracer atoms that penetrate the volume from the surface for a given annealing time (according to prior diffusion along grain boundaries) is roughly one half of the number of atoms that contribute to the broadening of layer II, and the condition  $J_v/J_g=2$  is valid, where  $J_v$  is the flux of atoms in bulk and  $J_g$  is the flux of atoms in grain boundaries, respectively. It is now assumed that the grains are approximately cubic with an average grain diameter of  $d=80$  nm and a grain boundary width of  $\delta=0.5$  nm. It is further assumed that  $J_i$  ( $i=v$  or  $g$ ) is given by  $J_i=A_i j_i$ , where  $A_i$  is the cross-section area of a grain and of a grain boundary perpendicular to the diffusion direction, and  $j_i$  is the corresponding flux density. The ratio of the respective areas is given by  $A_v/A_g \approx d/(2\delta)$  and we get  $j_v/j_g=4\delta/d$ . Using Fick's first law and the definition of the diffusion length,  $\Delta x \approx 2(D_i\Delta t)^{1/2}$ , the absolute value of  $j_i$  can be approximated as

$$j_i = D_i \left( \frac{\partial c}{\partial x} \right)_i \approx D_i \left( \frac{\Delta c}{\Delta x} \right)_i \approx \frac{\sqrt{D_i}}{2} \left( \frac{\Delta c}{\Delta t^{1/2}} \right)_i \quad (4)$$

which yields  $j_v/j_g \approx (D_v/D_g)^{1/2}$  for  $(\Delta c/\Delta t^{1/2})_v \approx (\Delta c/\Delta t^{1/2})_g$ , and  $D_g \approx D_v d^2/(4\delta)^2$ . Grain boundary diffusivities in the order of  $D_g \approx 10^3 D_v$  can be assessed which are quite reasonable. Note that for silicon nitride films with significantly larger grains the ratio  $J_v/J_g$  will increase (e.g., to about 250 for  $d=10$   $\mu\text{m}$ ) and the observed effect will be no longer visible due to the fact that fewer grain boundaries are present that may act as a transport path.

#### IV. DISCUSSION

For further analysis of the volume diffusivities given in Fig. 5, the equation

$$D_0 = f a^2 \nu_0 \exp\left(\frac{\Delta S}{k_B}\right) \quad (5)$$

is used, where  $f$  is the correlation factor,  $a$  the jump distance between two adjacent atoms,  $\nu_0$  the effective attempt frequency, and  $k_B$  the Boltzmann constant. From Eq. (5) the entropy of self-diffusion,  $\Delta S$ , can be assessed from the pre-exponential factor. Using  $a=0.26$  nm,  $f \approx 1$ , and  $\nu_0 \approx 10^{13}$  s $^{-1}$ , an entropy of  $\Delta S \approx (2 \pm 2) k_B$  is found for the diffusion in polycrystalline  $\text{Si}_3\text{N}_4$ . This value is in the same range as for metals and intermetallic compounds,<sup>12</sup> but it is lower, or at least at the lower limit of the values found for other semiconductors such as Si, Ge, or GaAs in the order of 5–10  $k_B$ .<sup>13,14</sup> These high entropy values are commonly explained by the presence of nonlocalized point defects (vacancies or self-interstitials) extended over several neighboring lattice sites.<sup>13</sup> This extended defect configuration may be realized by many microscopically different states with a high configuration entropy. The same is true for potential diffusion paths. However, the smaller entropy values for polycrystalline silicon nitride indicate that nitrogen and silicon are diffusing via localized point defects, more similar to conventional metals or intermetallics.

The present results on N diffusion can be compared to the data reported by Kijima and Shirasaki<sup>7</sup> in 1976 on reaction bonded silicon nitride powders, which are also shown in Fig. 5 for comparison. They used a gas-solid exchange method and measured the uptake of  $^{15}\text{N}$  gas in  $\alpha\text{-Si}_3\text{N}_4$  and  $\beta\text{-Si}_3\text{N}_4$  powders in a relatively limited temperature range between 1200 and 1400 °C. Volume diffusivities were determined by rescaling the data on powders with different particle size. Unexpected combinations and extremely large differences between the activation enthalpies (2.4 and 8.1 eV) and pre-exponential factors ( $1.2 \times 10^{-16}$  and  $1.9 \times 10^2$  m $^2$ /s) were found for the two  $\text{Si}_3\text{N}_4$  polymorphs. These diffusivities are some orders of magnitude lower and consequently in contradiction to the present data. We attribute the differences between the data of Kijima and Shirasaki and ours tentatively to a different chemical composition  $\text{SiN}_{1.33 \pm x}$  in the homogeneity range and/or to different levels of impurities present in the samples.

In order to search for a reliable self-diffusion mechanism in silicon nitride, several factors have to be considered: (i)

Atomic migration in crystalline solids commonly takes place with the help of point defects, which might be either vacancies or self-interstitials. The activation enthalpy of diffusion is then given by the sum of a formation,  $\Delta H^f$ , and of a migration part,  $\Delta H^m$ . (ii) In the intrinsic state, silicon nitride is an insulator with an electronic gap of about 5 eV.<sup>15</sup> Hence, charge neutrality has to be fulfilled, if charged defects are created. (iii) Similar or identical diffusivities in binary compounds indicate a common or coupled diffusion mechanism for both elements. (iv) The defect concentration governing diffusion does not depend on nitrogen partial pressure. From these facts, the following possible diffusion mechanism can be derived.

A coupled motion of both types of elements might be enforced by a Schottky type of defect. Such a defect consists of three silicon vacancies  $V_{\text{Si}}^{4-}$  and four nitrogen vacancies  $V_{\text{N}}^{3+}$  and charge neutrality is fulfilled for  $4[V_{\text{Si}}^{4-}] = 3[V_{\text{N}}^{3+}]$  (the square brackets indicate atomic fractions). A similar condition is valid for self-interstitials with  $4[I_{\text{Si}}^{4+}] = 3[I_{\text{N}}^{3-}]$ . In Ref. 16, the given defects are identified as the dominating ones compared to lower charged point defects (e.g.,  $V_{\text{Si}}^{3-}$ ) by a theoretical analysis of defect formation. If the charged interstitials are the dominating defect for diffusion, the formation enthalpy of a Schottky defect (sometimes also called anti-Schottky defect) is given by  $\Delta H_S^f = 3\Delta H^f(I_{\text{Si}}^{4+}) + 4\Delta H^f(I_{\text{N}}^{3-})$  and the nitrogen diffusivity is given by

$$D_{\text{N}} = D_0[I_{\text{N}}^{3-}] \exp(-\Delta H^m/k_B T) = D_0 \exp(-\Delta H_S^f/7k_B T) \times \exp(-\Delta H^m/k_B T). \quad (6)$$

Under the assumption that  $\Delta H^f \gg \Delta H^m$ , the activation enthalpy of diffusion is essentially determined by the defect formation enthalpy  $\Delta H = \Delta H^f$  and the silicon diffusivity is given by  $D_{\text{Si}} = 0.75 D_{\text{N}}$  due to charge neutrality. This will be in accordance with our experimental results given in Fig. 5. A negligible migration enthalpy might be due to the fact that the crystal structure of silicon nitride shows some type of cages or voids with a diameter of about 0.2–0.3 nm, where atomic motion may occur easily.<sup>17</sup> A similar mechanism is proposed for Si self-diffusion in quartz.<sup>18</sup> The same mechanism may in principle occur for vacancies, although a very small or similar migration enthalpy of N and Si vacancies would be more difficult to explain. As already stated in Sec. III, the formation of structural defects by a reaction with the nitrogen gas atmosphere do not seem to play a significant role here.

In case of neutral defects, charge neutrality has not necessarily to be fulfilled and vacancies or interstitials may be formed also independently. First-principles calculations on the point defect formation of neutral nitrogen vacancies in  $\text{SiN}_{1.33 \pm x}$  ( $x$ , small) were recently carried out by Tanaka *et al.* in the N-rich ( $x > 0$ ) and in the Si-rich ( $x < 0$ ) solution limit.<sup>19</sup> A strong variation of  $\Delta H^f$  between 6.5 eV and 3.8 eV for  $\alpha$ - $\text{Si}_3\text{N}_4$  and between 5.5 eV and 3.1 eV for  $\beta$ - $\text{Si}_3\text{N}_4$  was obtained for the N-rich and the Si-rich limit, respectively. This indicates a strong dependence of the diffusivities on the exact chemical composition and the chemical environment of the whole system. The relatively low value of  $\Delta H = \Delta H^f + \Delta H^m \approx 5$  eV found in this study has the consequence that a

low or nearly vanishing migration enthalpy is obtained also in case of neutral vacancies. Values in the range  $0 < \Delta H^m < 1.9$  eV might be possible, depending on the exact chemical composition.

Assuming a simple vacancy mechanism, a statistical motion of a vacancy via nearest neighbor jumps between the sublattices formed by the two types of elements is very unrealistic, because each moving vacancy would leave behind a tail of antisite defects. In order to enforce the equality of the diffusivities, migration via the same defect is a possibility, while the long range order is being restored. For instance, one could think of associated vacancy pairs ( $V_{\text{N}}V_{\text{Si}}$ ) or also interstitial pairs ( $I_{\text{N}}I_{\text{Si}}$ ).

Recently, we published a paper on nitrogen diffusion in magnetron sputtered amorphous silicon nitride layers with the same chemical composition as the crystalline layers investigated in this study.<sup>20</sup> These experiments were carried out with neutron reflectometry and  $\text{Si}_3^{14}\text{N}_4/\text{Si}_3^{15}\text{N}_4$  isotope multilayers. For the amorphous layers we found higher diffusivities than for the crystalline layers and a lower activation enthalpy of diffusion of only  $(3.6 \pm 0.4)$  eV while the corresponding pre-exponential factor is  $1 \times 10^{-9}$  m<sup>2</sup>/s. These data are also shown in Fig. 5 and can be discussed briefly in the context of the two possible diffusion mechanisms suggested for crystalline silicon nitride. As already stated, the quantity which dominates the activation enthalpy of diffusion for both mechanisms is the defect formation enthalpy,  $\Delta H^f$ . In order to explain consistently the experimental results this quantity has to be lower by 30% in amorphous silicon nitride. This can be understood with the fact that the amorphous structure is less closely packed compared to the crystalline structure and defect formation (and also migration) can be realized more easily.

It has to be mentioned that a completely other diffusion mechanism is also possible in amorphous silicon nitride in order to explain the low activation enthalpy of 3.6 eV. It can be assumed that the activation enthalpy of diffusion is identical to the migration enthalpy and consequently no significant thermal defect formation occurs.<sup>20</sup> Migration may take place with some kind of temperature independent structural defects, e.g., frozen in free volume which is formed during deposition with magnetron sputtering. These defects, however, will be removed completely during *in situ* crystallization and this mechanism cannot be assumed to take place in the crystalline state.

Unfortunately, this discussion can only be speculative due to the present poor knowledge of point defect formation and migration in silicon nitride.<sup>3</sup> Substantial theoretical and experimental work on that topic has to be carried out in order to achieve a consisting picture of the migration process of the constituting atoms.

## V. CONCLUSION

We used  $^{28}\text{Si}_3^{14}\text{N}_4/\text{nat}\text{Si}_3^{15}\text{N}_4/^{28}\text{Si}_3^{14}\text{N}_4$  isotope heterostructures and secondary ion mass spectrometry to determine the simultaneous diffusion of Si and N in polycrystalline silicon nitride, which is a model system for a covalently bound solid. In  $\alpha$ - $\text{Si}_3\text{N}_4$  we found very low diffusivities

( $10^{-23}$ – $10^{-18}$  m<sup>2</sup>/s), which are nearly identical for the two elements between 1200 and 1700 °C. Samples, composed of a mixture of  $\alpha$ -Si<sub>3</sub>N<sub>4</sub> and  $\beta$ -Si<sub>3</sub>N<sub>4</sub> show approximately the same N diffusivities, indicating that diffusion in both polymorphs is very similar. The self-diffusivities of the two elements follow a unique Arrhenius law with an activation enthalpy of  $\Delta H=5.0$  eV and a pre-exponential factor of  $D_0=6\times 10^{-6}$  m<sup>2</sup>/s. These results strongly suggest that the two atomic species are diffusing with a common or coupled diffusion mechanism. The small entropy of self-diffusion of  $\Delta S\approx 2 k_B$  shows that diffusion is mediated by localized point defects, in contrast to extended point defects usually

found in other semiconductors, like silicon, where a significantly higher value is expected. Possible diffusion mechanisms might be a coupled diffusion of the two atomic species via self-interstitials which are created by Schottky defect formation or, alternatively, a common diffusion via associated defect pairs such as, e.g., a double vacancies.

#### ACKNOWLEDGMENTS

The authors thank E. Ebeling for substrate preparation, M. Rudolphi and H. Baumann for carrying out the n-RBS measurements, and G. Borchardt for fruitful discussions.

- 
- <sup>1</sup>*Preparation and Properties of Silicon Nitride-Based Materials*, edited by D. A. Bonnell and T. Y. Tien, Materials Science Forum, Vol. 47 (Trans Tech Publ., Aedermannsdorf, 1989).
- <sup>2</sup>S. Hampshire, in *Materials Science and Technology*, edited by M. Swain, Vol. 11 (VCH, Weinheim, 1994), p. 122.
- <sup>3</sup>F. L. Riley, *J. Am. Ceram. Soc.* **83**, 245 (2000).
- <sup>4</sup>O. P. Agnihotri, S. C. Jain, J. Poortmans, J. Szlufcik, G. Beaucarne, J. Nijs, and R. Mertens, *Semicond. Sci. Technol.* **15**, R29 (2000).
- <sup>5</sup>F. H. P. M. Habraken and A. E. T. Kuiper, *Mater. Sci. Eng., R.* **12**, 123 (1994).
- <sup>6</sup>*Diffusion in Non-metallic Solids*, edited by D. L. Beke, Landolt-Börnstein New Series, Group III, Vol. 33 (Springer-Verlag, Berlin, 1999).
- <sup>7</sup>K. Kijima and S. Shirasaki, *J. Chem. Phys.* **65**, 2668 (1976).
- <sup>8</sup>K. P. Kunz, K. Sarin, R. F. Davis, and S. R. Bryan, *Mater. Sci. Eng., A* **105&106**, 47 (1988).
- <sup>9</sup>L. R. Doolittle, *Nucl. Instrum. Methods Phys. Res. B* **15**, 227 (1986).
- <sup>10</sup>H. Schmidt, G. Borchardt, M. Rudolphi, H. Baumann, and M. Bruns, *Appl. Phys. Lett.* **85**, 582 (2004).
- <sup>11</sup>H. Schmidt, W. Gruber, G. Borchardt, M. Bruns, M. Rudolphi, and H. Baumann, *Thin Solid Films* **450**, 344 (2004).
- <sup>12</sup>J. Philibert, *Atom Movements* (Les Editions de Physique, Les Ulis, 1991).
- <sup>13</sup>W. Frank, U. M. Gösele, H. Mehrer, and A. Seeger, *Diffusion in Crystalline Solids* (Academic Press, New York, 1984), p. 53.
- <sup>14</sup>H. D. Palfrey, M. Braun, and A. F. W. Willoughby, *J. Electrochem. Soc.* **128**, 2224 (1981).
- <sup>15</sup>R. Belkada, T. Shibayanagi, and M. Naka, *J. Am. Ceram. Soc.* **83**, 2449 (2000).
- <sup>16</sup>A. P. Garshin and V. E. Shvaiko-Shvaikovskii, *Refract. Ind. Ceram.* **39**, 169 (1998).
- <sup>17</sup>C.-M. Wang, X. Pan, M. Rühle, F. L. Riley, and M. Mitomo, *J. Mater. Sci.* **31**, 5281 (1996).
- <sup>18</sup>O. Jaoul, F. Béjina, and F. Élie, *Phys. Rev. Lett.* **74**, 2038 (1995).
- <sup>19</sup>I. Tanaka, K. Tatsumi, M. Nakano, H. Adachi, and F. Oba, *J. Am. Ceram. Soc.* **85**, 68 (2002).
- <sup>20</sup>H. Schmidt, M. Gupta, and M. Bruns, *Phys. Rev. Lett.* **96**, 055901 (2006).